This article has been accepted for publication in IEEE Photonics Journal. This is the author's version which has not been fully edited and content may change prior to final publication. Citation information: DOI 10.1109/JPHOT.2022.3206104

Wavelength-tuning of nanosecond pulses in Er-doped fluoride fibre amplifier

Paulami Ray, Amit Yadav, Solenn Cozic, Franck Joulain, Thibaud Berthelot, Ulf Hinze, Samuel Poulain, Edik U. Rafailov, and Nikolai B. Chichkov

***Abstract*—We investigate the gain bandwidth and wavelength-tuning range of an erbium-doped fluoride fibre amplifier. The presented experimental setup consisted of a widely wavelength-tunable optical parametric oscillator (OPO), which was amplified in a single-stage Er-doped fluoride fibre amplifier. The OPO laser provided seed pulses with a pulse width of 5.2 ns and a repetition rate of 10 kHz. The fibre section consisted of 2.2 m of double-clad, single-mode fibre with a doping concentration of 7 mol%. Wavelength-tuning was analysed at gain values of up to 26 dB and amplified pulse energies of up to 37.4 µJ. Using this setup, we demonstrate continuous wavelength tuning of more than 100 nm, covering the wavelength range from 2712 nm to 2818 nm.**

***Index Terms*—Fibre laser, Nanosecond, Erbium, Mid-infrared, ZBLAN, Fluoride fibre.**

I. Introduction

Erbium-doped fluoride fibre lasers provide high-power laser emission in the mid-infrared (MIR) at wavelengths around 2.8 µm. Their high average power levels, diffraction limited beam profiles, and emission wavelengths near the absorption maxima of biological and organic materials [1], have turned them into promising laser sources for a variety of applications in material processing [2], spectroscopy [3], and medicine [4]–[6]. This transition of fibre laser technology into the MIR was enabled by advances in the fabrication of fibres based on fluoride glasses [7], with low phonon energies and low-loss optical transmission in the entire MIR wavelength range. Er-doped fluoride fibre lasers now achieve output powers of up to 40 W [8] and pulse energies of several hundreds of microjoules [9]–[11].

Early research on Er-doped fluoride fibre lasers has been focussed on the development of laser oscillators, including continuous wave (CW) lasers [8], Q-switched lasers [10], [11], and mode-locked lasers [12]. More recently, several groups have demonstrated Er-doped fluoride fibre amplifiers for further power scaling of laser systems in the MIR. This included the generation of supercontinuum by amplification of picosecond pulses in a single-mode fibre amplifier at 2750 nm [13], the amplification of nanosecond pulses in a multi-mode fibre amplifier at 2710 nm [14], the amplification of 50 µJ pulses in a single-mode fibre amplifier at 2790 nm [15], and the demonstration of millijoule pulse energies from a dual-stage, multi-mode fibre amplifier at 2790 nm [16].

To develop new Er-doped fluoride fibre amplifier systems and to optimise the performance of existing setups, it is necessary to analyse their spectral characteristics, i.e. the gain bandwidth, accessible wavelength range, and the amplifier gain values versus laser wavelength. In theory, all optical parameters are well-known, i.e. emission/absorption cross-sections and rate equations, and numerical simulations of spectral properties should be possible. However, apart from solving the nonlinear rate equations in Er-doped fluoride fibres, numerical models would have to account for other effects that occur in experimental systems and affect the spectral characteristics, such as back-reflections from fibre end-caps [17], self-lasing [13], and potential amplified spontaneous emission (ASE). It is also not possible to simply rely on experimental results, which have been obtained by wavelength-tuning in Er-doped fluoride fibre oscillators [18]–[21]. Laser oscillators are typically operated at significantly higher saturation and lower single-pass gain values than fibre amplifiers. The peak emission wavelengths and accessible wavelength ranges of Er-doped fluoride fibre oscillators can therefore differ significantly from the ones obtained in fibre amplifiers. So far, no investigations, neither theoretical nor experimental, on the gain bandwidth and wavelength range accessible by Er-doped fluoride fibre amplifiers have been reported. A notable exception is the research of Duval et al. on wavelength-tuning of femtosecond pulses by nonlinear soliton self-frequency shift [22], [23]. However, this work focussed on nonlinear optical effects, which are not directly related to the gain distribution in Er-doped fibres.

In this paper, we present the experimental investigation of wavelength-tuning in a single-mode Er-doped fluoride fibre amplifier. By use of a widely tunable PPLN-based OPO, the entire emission range of Er-doped fluoride fibres can be investigated, enabling the analysis of the amplifier gain at different wavelengths and pump levels. To the best of our knowledge, this is the first investigation of wavelength-tuning in Er-doped fluoride fibre amplifiers, with the exception of nonlinear optical processes (i.e. supercontinuum, soliton shift).

II. Experimental setup

The experimental setup for the investigation of wavelength-tuning in Er-doped fluoride fibre amplifiers is illustrated in

This project has received funding from the European Union's Horizon 2020 research and innovation programme under the Marie Skłodowska-Curie grant agreement No 843801. This project has received funding from the Engineering and Physical Sciences Research Council (EPSRC), Grant No. EP/R024898/1.

N.B. Chichkov and U. Hinze are with the Institute of Quantum Optics, Leibniz University Hanover, Germany (email: n.chichkov@iqo.uni-hannover.de)

P. Ray, A. Yadav, E.U. Rafailov, and N.B. Chichkov are with the Aston Institute of Photonic Technologies, Aston University, Birmingham, UK.

U. Hinze is with the Laser nanoFab GmbH, Hanover, Germany.

S. Cozic, F. Joulain, T. Berthelot, and S. Poulain are with Le Verre Fluoré, Campus KerLann, Bruz, France.

This work is licensed under a Creative Commons Attribution 4.0 License. For more information, see https://creativecommons.org/licenses/by/4.0/

This article has been accepted for publication in IEEE Photonics Journal. This is the author's version which has not been fully edited and
content may change prior to final publication. Citation information: DOI 10.1109/JPHOT.2022.3206104

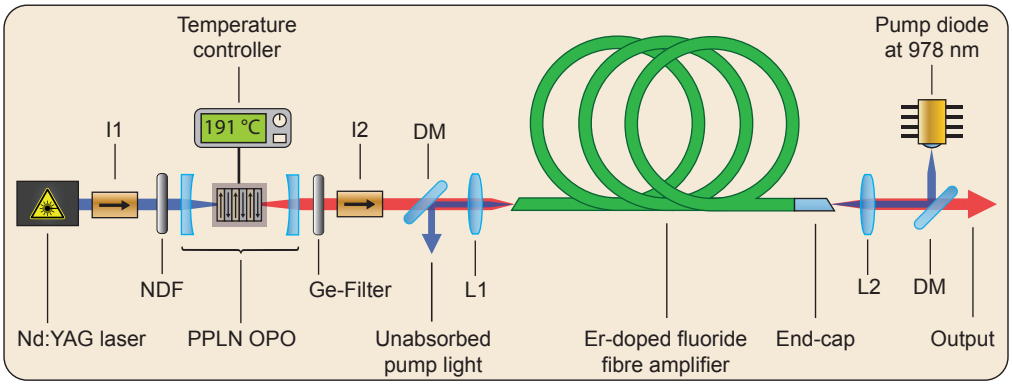

Fig. 1. Experimental setup (from left to right): (i) Q-switched Nd:YAG pump laser, (ii) PPLN-based OPO with temperature control for non-critical phase-matching, (iii) Er-doped fluoride fibre amplifier. I1: isolator at 1064 nm; NDF: neutral density filter wheel; I2: isolator at 2750 nm; DM: dichroic mirror HT at 2800 nm and HR at 980 nm; L1: CaF_2 lens, $f = 25$ mm; L2: CaF_2 lens, $f = 20$ mm.

Fig. 1. The setup consisted of two parts: a PPLN-based OPO and a single-stage Er-doped fluoride fibre amplifier. The OPO generated wavelength-tunable seed laser pulses, which were used to characterise the fibre amplifier over the entire wavelength range from 2700–2850 nm. The OPO was pumped by an actively Q-switched Nd:YAG laser, operating at a wavelength of 1064 nm with a repetition rate of 10 kHz. A neutral density filter wheel (NDF) was placed at the output of the Nd:YAG laser, enabling fine adjustment of the OPO pump power. The nonlinear medium in the OPO was a 5% MgO-doped PPLN-crystal with seven grating periods ranging from 28.5 to 31.5 μm. The crystal was placed in a temperature controlled oven to achieve wavelength conversion by non-critical phase-matching. To generate idler output at wavelengths from 2700–2850 nm, the 31 µm and 31.5 µm grating periods were utilised and the oven temperature was modified between 100 °C to 200 °C. A germanium filter was used to block unwanted OPO output at wavelengths below 2 µm (signal and pump).

The fiber amplifier consisted of a single section of double-clad Er-doped fluoride fibre, pumped in counter-propagating direction with a multi-mode laser diode operating at 978 nm. The fibre, manufactured by Le Verre Fluoré, had a length of 2.2 m and a doping concentration of 7 mol%. The pump-cladding had a diameter of 260 µm, a numerical aperture (NA) of 0.46, and a double-D shape with two parallel flats at a distance of 240 µm. The fibre core had a diameter of 15.5 µm and a NA of 0.125, corresponding to a cut-off wavelength of 2.5 µm for single-mode operation. Background losses in the fibre core result in an attenuation value of 21 dB/km for light propagation at a wavelength of 2.8 µm. The theoretical saturation power of the fibre gain medium was calculated to 5.6 mW [23].

The output facet of the fibre was protected with a fluoroaluminate (AlF_3) end-cap to suppress degradation from O-H diffusion and to prevent fibre damage at high output powers after amplification. The fibre ends were angle-cleaved at 4°(input) and 13°(output), to reduce back-reflections and suppress self-lasing in the fibre section—the difference in cleaving angles was due to tolerances in the cleaving process.

An optical isolator, optimised for a wavelength of 2750 nm, was placed between the OPO and the fibre amplifier to block back-reflections and suppress feedback. The seed laser was coupled with an uncoated, plano-convex CaF_2 lens ($f = 25$ mm) into the fibre section. A second plano-convex CaF_2 lens ($f = 20$ mm) was used to collimate the amplifier output and to couple the pump laser into the fibre cladding. The pump laser was injected with a dichroic mirror (DM) into the fibre amplifier—transmission above 97 % at 2800 nm and reflectivity above 99.5 % at 978 nm. A second dichroic mirror was used at the opposite end of the fibre section to remove the unabsorbed pump light.

The OPO laser provided seed pulses with an average power of 2.7 mW, a pulse energy of 270 nJ, and pulse duration of 5.2 ns (measured with a photodiode rise-time of 3.5 ns). After transmission losses (isolator, lenses, DM) and fibre coupling, we measured an average power of 0.9 mW at the output of the fibre amplifier, corresponding to a total coupling efficiency of 30 % into the single-mode fibre core. Throughout the experiments the seed power inside the fibre core was kept constant at 0.9 mW, to ensure identical conditions in the fibre amplifier at all investigated wavelengths. Minor changes in the fibre coupling efficiency at different seed laser wavelengths, were compensated by adjustment of the OPO pump power.

The spectrum of the amplified laser pulses was characterised with a Horiba iHR-550 monochromator in combination with an amplified PbSe photodetector (Thorlabs PDA20H) and a lock-in amplifier. The spectra were measured with a nominal

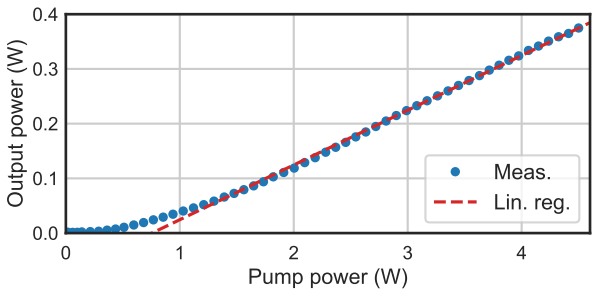

Fig. 2. Amplified output power versus pump power (blue, dots) and linear regression above 1 W (red, dashed).

This work is licensed under a Creative Commons Attribution 4.0 License. For more information, see https://creativecommons.org/licenses/by/4.0/

This article has been accepted for publication in IEEE Photonics Journal. This is the author's version which has not been fully edited and
content may change prior to final publication. Citation information: DOI 10.1109/JPHOT.2022.3206104

slit size of 40 µm, corresponding to a theoretical resolution of less than 0.2 nm. All spectra were recorded over the entire wavelength range from 2710 nm to 2850 nm to check for the appearance of self-lasing spikes. The temporal pulse profile was measured with a fast HgCdTe photodiode (Thorlabs PDAVJ10) with a response bandwidth of 100 MHz and a theoretical rise-time of 3.5 ns.

All experiments were performed in a temperature-stabilised laboratory environment. The beam path and free-space sections were not shielded from the laboratory atmosphere and not purged with Nitrogen. This resulted in strong modulations of the laser spectra due to atmospheric absorptions located within the investigated wavelength range.

III. Results

The highest output power and amplifier gain were obtained at a laser wavelength of 2790 nm. The amplified output power versus launched pump power is plotted in Fig. 2. The maximum output power of 375 mW was obtained at a pump power of 4.5 W, corresponding to a pulse energy of 37.5 µJ and a gain of 26.2 dB inside the fibre amplifier, i.e. calculated for the seed power of 0.9 mW and excluding transmission and coupling losses between the OPO and the fibre amplifier. At this output power an optical efficiency of 8.3 % and a slope efficiency of 10.0 % were achieved. The fibre amplifier was fully saturated. Further amplification was limited by the onset of self-lasing in the fibre section.

The evolution of the amplified pulse spectrum at different output power levels is shown in Fig. 3. The seed pulse from the OPO had a peak wavelength of 2790 nm and a bandwidth of 10.0 nm (full-width at $1/e^2$). The spectral shape of the pulse remained consistent during amplification, however, at higher output powers the amplified laser spectrum began to exhibit signs of nonlinear spectral broadening. At the maximum output power of 375 mW, the spectrum had a bandwidth of 16.7 nm and a peak wavelength of 2789 nm. The recorded spectrum exhibited no signs of self-lasing or ASE over the wavelength range of 2710–2850 nm. Finally, Fig. 4 shows the temporal pulse profile of the amplified laser pulse at the maximum output power of 375 mW. The pulse had a duration of 5.2 ns (full-width at half-maximum, FWHM), corresponding to a peak power of 5.7 kW. The inset of Fig. 4 also shows she amplified pulse train, which was recorded over a period of 4 ms (i.e. 40 successive pulses). The pulse train had pulse energy fluctuations of 6.7 % (standard deviation), resulting from comparable fluctuations (standard deviation of 5.4 %) of the seed pulses provided by the OPO.

The operation state of the fibre amplifier at the laser wavelength of 2789 nm was used as starting point for the investigation of wavelength-tuning. By variation of the selected grating period and of the PPLN-crystal temperature, the wavelength of the seed pulses from the OPO was tuned from 2712 nm to 2818 nm in increments of 6–8 nm (corresponding to 2 °C steps in the PPLN temperature). It must be noted, however, that the peak wavelength of the amplified laser pulses did not exactly coincide with the peak wavelength of the seed pulses—minor shifts in peak wavelength of up to 2 nm were observed

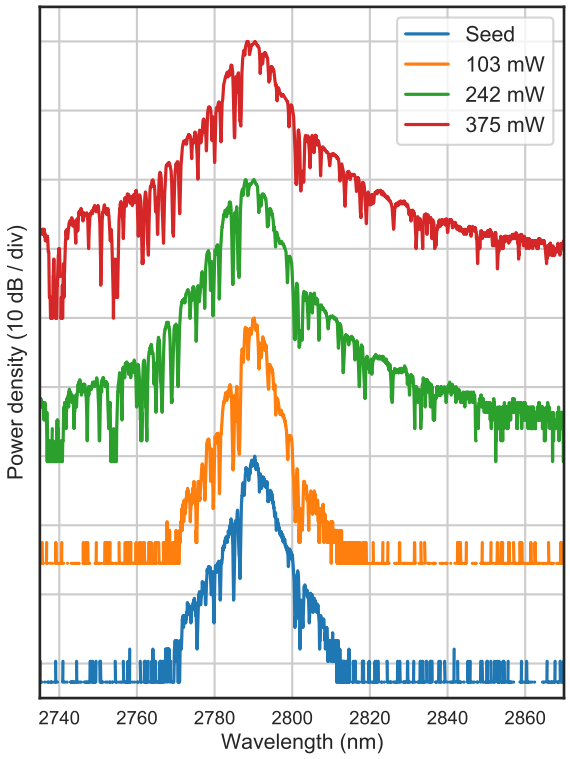

Fig. 3. Seed laser spectrum and amplified laser spectrum at different output power levels.

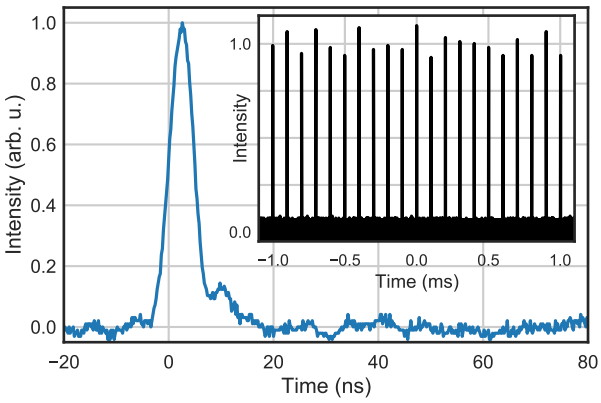

Fig. 4. Measured temporal pulse profile and series of 20 successive pulses (inset).

after amplification. Fig. 5 shows the amplified output power versus the peak wavelength of the amplifier output at different pump power levels. At a pump power of 1.8 W, a maximum output power of 121 mW was obtained at a wavelength of 2773 nm, which corresponds to an amplifier gain of 21.3 dB. The output power and gain remained almost constant over the entire wavelength range from 2712 nm to 2797 nm. Output powers of 96 mW (20.3 dB gain) and 108 mW (20.8 dB gain) were obtained at 2712 nm and 2797 nm, respectively. At longer wavelengths, beyond 2800 nm, the amplified output power began to decrease, dropping to a value of 36 mW (16.0 dB gain) at a wavelength of 2818 nm. This corresponds to a total wavelength-tuning range of 106 nm from 2712 nm

This work is licensed under a Creative Commons Attribution 4.0 License. For more information, see https://creativecommons.org/licenses/by/4.0/

This article has been accepted for publication in IEEE Photonics Journal. This is the author's version which has not been fully edited and
content may change prior to final publication. Citation information: DOI 10.1109/JPHOT.2022.3206104

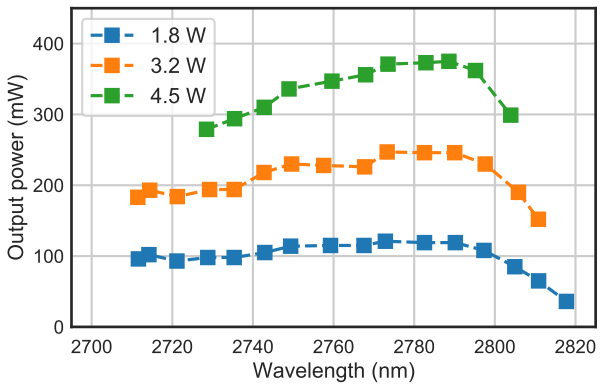

Fig. 5. Amplified output power versus peak laser wavelength at different pump powers and amplifier gain levels. The pump powers of 1.8 W, 3.2 W, and 4.5 W corresponded to peak amplifier gain values of 21.3 dB, 24.4 dB, and 26.2 dB, respectively.

to 2818. Further wavelength-tuning was limited by the onset of self-lasing in the fibre section, occurring at seed laser wavelengths below 2712 nm and above 2818 nm. The amplified laser spectra at different wavelengths for the pump power of 1.8 W are shown in Fig. 6. The width of the laser spectrum, remained mostly unchanged over the complete wavelength-tuning range. However, the spectra exhibited pronounced modulations (dips) as the spectrum was scanned across different atmospheric absorption lines—e.g. around 2720 nm, 2740 nm, and 2754 nm.

At a pump power of 3.2 W, the maximum output power increased to 247 mW and was obtained at an amplified laser wavelength of 2773 nm, corresponding to a gain value of 24.4 dB. The amplifier gain and output power remained stable over the wavelength-tuning range of 2712–2798 nm, resulting in an output power of 183 mW (23.1 dB) at 2712 nm and 230 mW (24.1 dB) at 2798 nm. The increase of the laser wavelength to 2812 nm resulted in an output power of 152 mW and an amplifier gain of 22.3 dB. Further wavelength-tuning was limited by self-lasing in the fibre section.

At the maximum pump power of 4.5 W, the peak gain shifted to a wavelength of 2789 nm—output power of 375 mW and gain value of 26.2 dB. The wavelength-tuning range decreased to 76 nm—covering wavelengths from 2728 nm to 2804 nm— and was again limited by self-lasing in the fibre section. At the wavelength of 2728 nm an output power of 279 mW and an amplifier gain of 24.9 dB were obtained. At the wavelength of 2804 nm, the amplifier provided an output power of 299 mW, corresponding to a gain of 25.2 dB. The amplified laser spectra at different wavelengths are plotted in Fig. 7. All spectra had an increased bandwidth and a symmetric power transfer to the wings of the spectrum could be observed. This change in spectral characteristics can be explained by self-phase-modulation (SPM) inside the fibre section at peak powers of up to 5.7 kW [23]. The main features of the amplified laser spectra remained similar across the entire tuning range. Differences in the shape and modulation of the laser spectra, resulted again from atmospheric absorption lines in the investigated wavelength range.

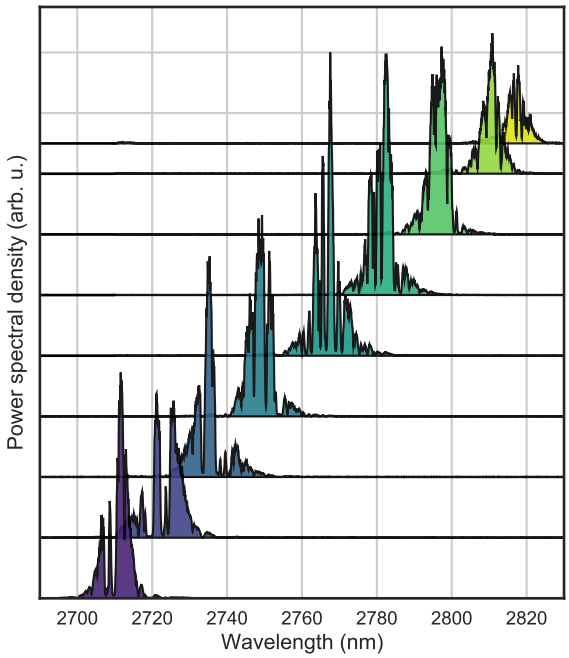

Fig. 6. Wavelength-tuning in Er-doped fluoride fibre amplifier from 2712 nm to 2818 nm at a pump power level of 1.8 W.

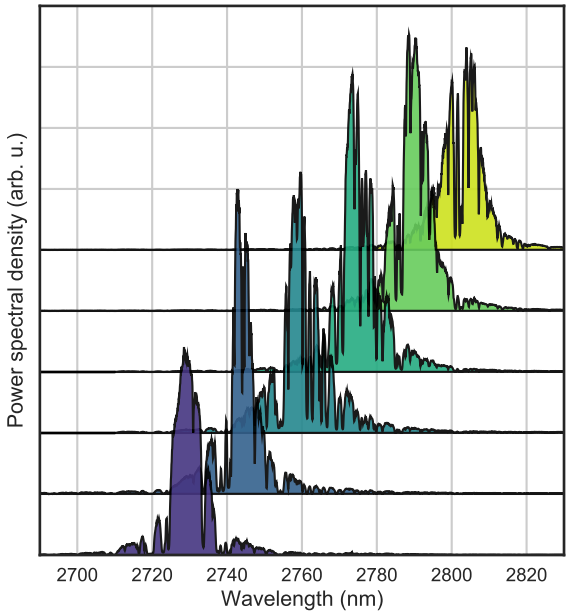

Fig. 7. Wavelength-tuning in Er-doped fluoride fibre amplifier from of 2728 nm to 2884 nm at a pump power level of 4.5 W.

The observed shift of the gain maximum from 2773 nm at a pump power of 1.8 W to 2789 nm at the maximum pump power of 4.5 W can be explained by changes in the population densities of the upper and lower laser levels of the Er^{3+}-ions [7], [23]. The Er^{3+}-ions act as four-level gain medium with an initially unpopulated lower laser level. As the laser power increases, more Er^{3+}-ions are transferred to the lower laser level through stimulated emission. In combination with the long lifetime of the lower laser level of 9.9 ms, this leads to

This work is licensed under a Creative Commons Attribution 4.0 License. For more information, see https://creativecommons.org/licenses/by/4.0/

This article has been accepted for publication in IEEE Photonics Journal. This is the author's version which has not been fully edited and content may change prior to final publication. Citation information: DOI 10.1109/JPHOT.2022.3206104

an increase in the populations density of the lower laser level, which causes reabsorption of the laser signal and results in a shift of the gain maximum to longer wavelengths.

The presented experiments were performed over a period of two weeks. During this time frame, no degradation of the laser performance was observed. The fibre amplifier was operated only for short time intervals of 30–60 min to avoid degradation of the fibre facets [17].

The obtained results demonstrate the broad gain bandwidth of Er-doped fluoride fibre amplifiers. The main limitation to wavelength-tuning, that has been observed in the presented amplifier setup, is the onset of self-lasing, which arises from Fresnel back-reflections at the AlF_3 end-cap and fibre facets. In theory, wavelength tuning should be possible across the entire gain bandwidth of the Er-doped fluoride fibre, corresponding to wavelength ranges of more than 170 nm [20]. However, tuning of the seed laser wavelength to shorter or longer wavelengths, away from the gain maximum, results in a decrease of the effective amplifier gain. This in turn leads to a reduced saturation of the fibre amplifier and an increase of the residual (saturated) small-signal gain value at wavelengths near the gain maximum. Self-lasing in the fibre section occurs, if this gain becomes sufficient to amplify back-reflections from the fibre facets over one round-trip.

The onset of self-lasing in the fibre section is also the main limitation on further power scaling, limiting the maximum achievable single-pass gain values to 25–30 dB [13], [15]. Improvement of the end-cap design and a further increase of cleaving angles are required to reduce back-reflections and suppress the onset of self-lasing. This is expected to enable broader wavelength-tuning ranges and further power scaling.

IV. Conclusion

We have used the idler output from a wavelength-tunable PPLN-based OPO to investigate the gain distribution and accessible wavelength range of a single-mode Er-doped fluoride fibre amplifier. We demonstrated the amplification of nanosecond pulses with pulse energies of up to 37.5 µJ and amplifier gain values of 26.2 dB at a wavelength of 2789 nm. The peak wavelength of the amplified laser pulses was tuned over a range of 76 nm, limited only by self-lasing in the fibre section. Over the entire wavelength range an amplifier gain of more than 25 dB was obtained. Even broader wavelength-tuning ranges of up to 106 nm have been achieved at lower amplifier gain values of 16.0–21.3 dB.

This is the first experimental investigation of wavelength-tuning in Er-doped fluoride fibre amplifiers and the obtained results show the potential for the development of high-power laser sources with broad wavelength-tuning ranges of more than 100 nm. Further research must focus on the suppression of self-lasing in the fibre section to allow for higher amplifier gain values and wider wavelength-tunability. Promising applications include the combination of broadband Er-doped fluoride fibre amplifiers with compact wavelength-tunable semiconductor laser devices in the MIR [24].

References

[1] J. E. Bertie and Z. Lan, "Infrared Intensities of Liquids XX: The Intensity of the OH Stretching Band of Liquid Water Revisited, and the Best Current Values of the Optical Constants of H_2O(l) at 25°C between 15,000 and 1 cm^{-1}," *Applied Spectroscopy*, vol. 50, no. 8, pp. 1047–1057, Aug. 1996.

[2] C. Frayssinous, V. Fortin, J.-P. Bérubé, A. Fraser, and R. Vallée, "Resonant polymer ablation using a compact 3.44µm fiber laser," *Journal of Materials Processing Technology*, vol. 252, pp. 813–820, Feb. 2018.

[3] N. Picqué and T. W. Hänsch, "Mid-IR Spectroscopic Sensing," *Optics and Photonics News*, vol. 30, no. 6, pp. 26–33, Jun. 2019.

[4] M. Skorczakowski, J. Swiderski, W. Pichola, P. Nyga, A. Zajac, M. Maciejewska, L. Galecki, J. Kasprzak, S. Gross, A. Heinrich, and T. Bragagna, "Mid-infrared Q-switched Er:YAG laser for medical applications," *Laser Physics Letters*, vol. 7, no. 7, p. 498, May 2010.

[5] M. C. Pierce, S. D. Jackson, M. R. Dickinson, T. A. King, and P. Sloan, "Laser-tissue interaction with a continuous wave 3-µm fibre laser: Preliminary studies with soft tissue," *Lasers in Surgery and Medicine*, vol. 26, no. 5, pp. 491–495, 2000.

[6] L. Hympanova, K. Mackova, M. El-Domyati, E. Vodegel, J.-P. Roovers, J. Bosteels, L. Krofta, and J. Deprest, "Effects of non-ablative Er:YAG laser on the skin and the vaginal wall: systematic review of the clinical and experimental literature," *International Urogynecology Journal*, vol. 31, no. 12, pp. 2473–2484, Dec. 2020.

[7] S. D. Jackson, "Towards high-power mid-infrared emission from a fibre laser," *Nature Photonics*, vol. 6, no. 7, pp. 423–431, Jul. 2012.

[8] Y. O. Aydin, V. Fortin, R. Vallée, and M. Bernier, "Towards power scaling of 28 µm fiber lasers," *Optics Letters*, vol. 43, no. 18, p. 4542, Sep. 2018.

[9] X. Zhu, G. Zhu, C. Wei, L. V. Kotov, J. Wang, M. Tong, R. A. Norwood, and N. Peyghambarian, "Pulsed fluoride fiber lasers at 3 µm [Invited]," *Journal of the Optical Society of America B*, vol. 34, no. 3, p. A15, Mar. 2017.

[10] S. Tokita, M. Murakami, S. Shimizu, M. Hashida, and S. Sakabe, "12W Q-switched Er:ZBLAN fiber laser at 28 µm," *Optics Letters*, vol. 36, no. 15, p. 2812, Aug. 2011.

[11] P. Paradis, V. Fortin, Y. O. Aydin, R. Vallée, and M. Bernier, "10 W-level gain-switched all-fiber laser at 28 µm," *Optics Letters*, vol. 43, no. 13, p. 3196, Jul. 2018.

[12] S. Duval, M. Bernier, V. Fortin, J. Genest, M. Piché, and R. Vallée, "Femtosecond fiber lasers reach the mid-infrared," *Optica*, vol. 2, no. 7, pp. 623–626, Jul. 2015, publisher: Optica Publishing Group.

[13] J.-C. Gauthier, V. Fortin, S. Duval, R. Vallée, and M. Bernier, "In-amplifier mid-infrared supercontinuum generation," *Optics Letters*, vol. 40, no. 22, pp. 5247–5250, Nov. 2015.

[14] W. Du, X. Xiao, Y. Cui, J. Nees, I. Jovanovic, and A. Galvanauskas, "Demonstration of 067-mJ and 10-ns high-energy pulses at 272 µm from large core Er:ZBLAN fiber amplifiers," *Optics Letters*, vol. 45, no. 19, p. 5538, Oct. 2020.

[15] N. B. Chichkov, P. Ray, S. Cozic, A. Yadav, F. Joulain, S. V. Smirnov, U. Hinze, S. Poulain, and E. U. Rafailov, "Amplification of nanosecond pulses in a single-mode erbium-doped fluoride fibre amplifier," *IEEE Photonics Technology Letters*, pp. 1–1, 2022.

[16] Y. O. Aydin, Y. O. Aydin, S. Magnan-Saucier, D. Zhang, V. Fortin, D. Kraemer, R. Vallée, and M. Bernier, "Dual stage fiber amplifier operating near 3 µm with milijoule-level, sub-ns pulses at 5 W," *Optics Letters*, vol. 46, no. 18, pp. 4506–4509, Sep. 2021.

[17] Y. O. Aydin, F. Maes, V. Fortin, S. T. Bah, R. Vallée, and M. Bernier, "Endcapping of high-power 3 µm fiber lasers," *Optics Express*, vol. 27, no. 15, p. 20659, Jul. 2019.

[18] X. Zhu and R. Jain, "Compact 2 W wavelength-tunable Er:ZBLAN mid-infrared fiber laser," *Optics Letters*, vol. 32, no. 16, pp. 2381–2383, Aug. 2007, publisher: Optica Publishing Group.

[19] S. Tokita, M. Hirokane, M. Murakami, S. Shimizu, M. Hashida, and S. Sakabe, "Stable 10 W Er:ZBLAN fiber laser operating at 2.71–2.88µm," *Optics Letters*, vol. 35, no. 23, pp. 3943–3945, Dec. 2010, publisher: Optica Publishing Group.

[20] C. Wei, H. Luo, H. Shi, Y. Lyu, H. Zhang, and Y. Liu, "Widely wavelength tunable gain-switched Er^{3+}-doped ZBLAN fiber laser around 2.8 µm," *Optics Express*, vol. 25, no. 8, pp. 8816–8827, Apr. 2017, publisher: Optica Publishing Group.

[21] C. Wei, H. Zhang, H. Shi, K. Konynenbelt, H. Luo, and Y. Liu, "Over 5-W Passively Q-Switched Mid-Infrared Fiber Laser With a Wide Continuous Wavelength Tuning Range," *IEEE Photonics Technology Letters*, vol. 29, no. 11, pp. 881–884, Jun. 2017, conference Name: IEEE Photonics Technology Letters.

This work is licensed under a Creative Commons Attribution 4.0 License. For more information, see https://creativecommons.org/licenses/by/4.0/

This article has been accepted for publication in IEEE Photonics Journal. This is the author's version which has not been fully edited and content may change prior to final publication. Citation information: DOI 10.1109/JPHOT.2022.3206104

[22] S. Duval, J.-C. Gauthier, L.-R. Robichaud, P. Paradis, M. Olivier, V. Fortin, M. Bernier, M. Piché, and R. Vallée, "Watt-level fiber-based femtosecond laser source tunable from 2.8 to 3.6 μm," *Optics Letters*, vol. 41, no. 22, pp. 5294–5297, Nov. 2016, publisher: Optica Publishing Group.

[23] S. Duval, M. Olivier, L.-R. Robichaud, V. Fortin, M. Bernier, M. Piché, and R. Vallée, "Numerical modeling of mid-infrared ultrashort pulse propagation in Er^{3+}: fluoride fiber amplifiers," *JOSA B*, vol. 35, no. 6, pp. 1450–1462, Jun. 2018, publisher: Optical Society of America.

[24] N. B. Chichkov, A. Yadav, E. Zherebtsov, M. Wang, G. Kipshidze, G. Belenky, L. Shterengas, and E. U. Rafailov, "Wavelength-Tunable, GaSb-Based, Cascaded Type-I Quantum-Well Laser Emitting Over a Range of 300 nm," *IEEE Photonics Technology Letters*, vol. 30, no. 22, pp. 1941–1943, Nov. 2018.

This work is licensed under a Creative Commons Attribution 4.0 License. For more information, see https://creativecommons.org/licenses/by/4.0/